4th International Conference on vortex flows and models (ICVFM2008)
21-23 April 2008, Daejeon, Korea

# An Analysis of Transient Motion and Characteristics of Screech Tone in Three Dimensional Simulations

I.C. Lee,[*1] and D.J. Lee, [*2]

*1 Department of Mechanical Engineering, KAIST, Daejeon 305-701, Korea
E-mail: essence@kaist.ac.kr
*2 Department of Mechanical Engineering, KAIST, Daejeon 305-701, Korea
E-mail: djlee@kaist.ac.kr

**ABSTRACT:** In this work, the screech tone of an underexpanded jet is numerically calculated. To make a successful analysis of screech tone, we use the method of CAA (computational aeroacousitcs), which has high-resolution and high-order. In this work, we use fourth-order OHOC (optimized high-order compact) schemes for the evaluation of spatial derivatives and the fourth-order Runge-Kutta scheme for the integration in time. We have simulated the screech tone of axisymmetric mode and three dimensional mode numerically and the results are compared with other numerical results and experimental results. When the jet Mach number is relatively law, the supersonic jet flow generated screech tone of axisymmetric mode after transient behavior. As the jet Mach number increases, the supersonic jet flow starts to generate the screech tone of three dimensional mode. However, at the initial stage, both the jet flow and the screech tone show axisymmetry even for higher jet Mach number. And the characteristics of asymmetry and three dimensional screech tone are shown as computational time increases. The interaction between vortices and shock cells at the initial stage and the interaction between vortices and shock cells at the later time which shows three dimensional effect are compared each other. The azimuthal variation of three dimensional screech tone is investigated. Two modes can be observed in three dimensional analysis. One is known as B mode, the other is known as C mode. Both B mode and C mode are observed at jet Mach number 1.43 and their azimuthal directivity is also observed. It is observed that the directivities of both B mode and C mode is similar with the directivity of dipole source, however their main directivities or maximum flapping planes are perpendicular to each other.

**KEYWORDS**: Screech tone, jet noise, computational aeroacoustics and feedback

## 1. INTRODUCTION

When supersonic jet flow is generated, jet noise is also generated from the jet flow. Supersonic jet noise has clear directivity patterns depending on the noise component. Supersonic jet noise consists of three principal components: turbulent mixing noise, broadband-shock-associated noise, and screech tones [1]. Turbulent mixing noise radiates downstream due to a large-scale turbulence structure as a supersonic Mach wave. Shock-associated noise and screech tone propagate upstream due to shock cell structure, which are only generated by under-expanded jet. Shock-associated noise is produced by the interaction between a shock cell and a vortex, whereas screech tone is produced by a feedback loop near the nozzle exit.

For over fifty years, research on screech tone has been conducted via experimental and theoretical methods. Numerical simulations have been widely used recently because numerical computation has become so powerful. One of the common methods is turbulent modeling [2-3]. The other method is direct numerical simulation (DNS) [4]. Large eddy simulation (LES) [5] is another method which can simulate jet noise numerically. However, the characteristics of screech tone and its transient behavior at the initial stage have not been investigated by neither experiments nor numerical simulations. So, additional investigations on when the screech tone begins to be generated and how the screech tone becomes periodic are necessary.

In this work, an underexpanded supersonic jet with Mach number 1.10, 1.15, 1.18 and 1.43 is numerically calculated from the initial stage to investigate the transient behavior of the screech tone after validation of present method. The interaction between vortices and shock cells at the initial stage and the interaction between vortices and shock cells at the later time which shows three dimensional effect are compared each other at each Mach number. The azimuthal variation of three dimensional screech tone is investigated. The directivity of three dimensional screech tone is investigated at the jet Mach number of 1.43.

## 2. GOVERNING EQUATIONS AND NUMERICAL METHODS

In this work three dimensional Euler equation is used and no effect of viscous flow is considered. All the governing equations of motion for the axisymmetric inviscid flow are:

$$\frac{\partial \mathbf{Q}}{\partial t} + \frac{\partial \mathbf{E}}{\partial x} + \frac{\partial \mathbf{F}}{\partial y} + \frac{\partial \mathbf{G}}{\partial z} = 0 \tag{1}$$

where

$$\mathbf{Q} = \begin{bmatrix} \rho \\ \rho u \\ \rho v \\ \rho w \\ \rho e_t \end{bmatrix}, \mathbf{E} = \begin{bmatrix} \rho u \\ \rho u^2 + p \\ \rho uv \\ \rho uw \\ (\rho e_t + p)u \end{bmatrix}, \mathbf{E} = \begin{bmatrix} \rho v \\ \rho vu \\ \rho v^2 + p \\ \rho vw \\ (\rho e_t + p)v \end{bmatrix}, \mathbf{G} = \begin{bmatrix} \rho w \\ \rho wu \\ \rho wv \\ \rho w^2 + p \\ (\rho e_t + p)w \end{bmatrix} \tag{2}$$

To accurately simulate a screech tone, the flow near the nozzle exit should be simulated correctly and the wave, which propagates upstream with relatively small amplitude, should be analyzed precisely. Hence to successfully analyze a screech tone, the method of CAA (computational aeroacousitcs), which has high-resolution and high-order is used. In this work, fourth-order OHOC (optimized high-order compact) [6-7] schemes for the evaluation of spatial derivatives and the fourth-order Runge-Kutta scheme for the integration in time are used. The adaptive nonlinear artificial dissipation model [8] is also used to remove unwanted numerical dissipation. Generalized characteristic boundary conditions [9] and absorbing layer, which is shown as gray thick line along the boundary in Fig. 1, are used as the time-dependent boundary conditions to prevent unwanted non-physical reflections around the computational boundaries. Fig. 1 shows the entire computation domain schematically. The domain consists of three sub-domains. The numerical domain extends 50 times the nozzle exit diameter in the x direction and 30 times the nozzle exit diameter in the y direction. The total number of grid points on two dimensional plane is about 100,000 including absorbing layer and grid points are condensed around the nozzle exit both in the x and y directions. There are 48 grid points in azimuthal direction. Totally 4,800,000 grid points are used for three dimensional computation.

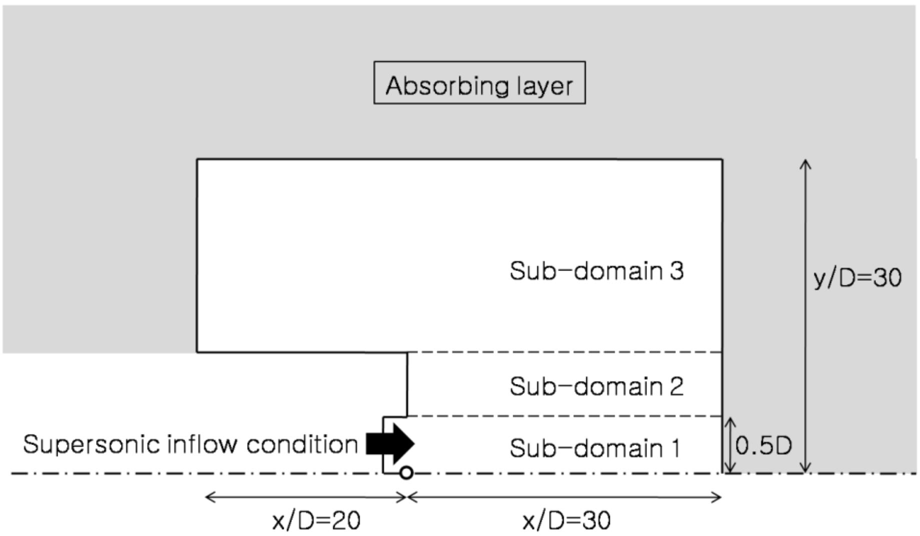


Fig. 1 Schematic view of computational domain and boundary conditions

Initially, the whole computational domain is set to ambient flow conditions and the supersonic inflow condition at the nozzle exit is specified as follows [10] with the use of ideal gas isentropic relations:

$$p = \frac{1}{\gamma}\left[\frac{2+(\gamma-1)M^2}{\gamma+1}\right]^{\frac{\gamma}{\gamma-1}}$$

$$\rho = \frac{\gamma(\gamma+1)p}{2T_r} \qquad (3)$$

$$u = \left(\frac{2T_r}{\gamma+1}\right)^{\frac{1}{2}},\ v = 0$$

In this research, $T_r$ is equal to 1, because only cold jet condition is considered in this work.

## 3. NUMERICAL RESULTS

### 3.1 Validation

We have numerically simulated the supersonic jet flow with jet Mach number 1.76 to validate the developed method. Generally, the axisymmetry of the jet flow breaks down and the jet flow shows three dimensional characteristics when the jet Mach number is greater than 1.20. To observe the initial behavior of supersonic jet flow, a time history is measured at specific location. The numerically measured time history signal at the initial stage is compared with experimental and numerical results performed by Wang and Widhopf[11]. It is also compared with the result of two dimensional calculation.

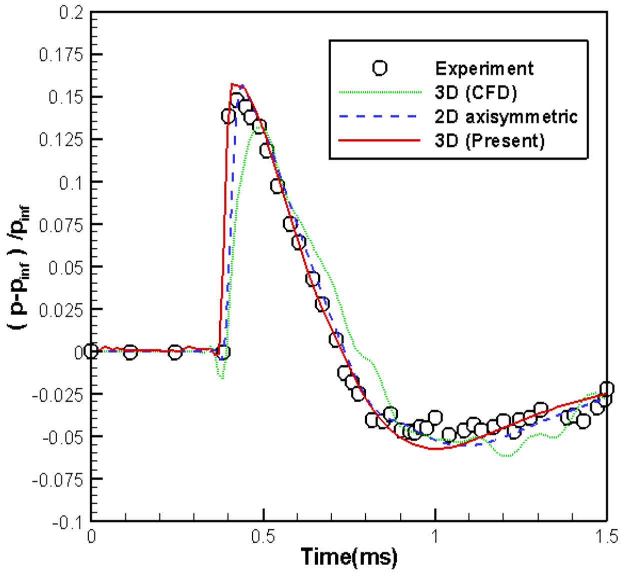


Fig. 2 Pressure signal at the plane of nozzle exit(x/D=0.012, y/D=1.49)

Fig. 2 shows the comparison of pressure signal at one position of the nozzle exit plane (x/D=0.012, y/D=1.49). The experimental data (circular symbol) and three dimensional CFD data (green line) are the result of Wand and Widhopf. And the two dimensional axisymmetric data (dashed line) and three dimensional data (red line) are the result of present work. The present result shows a better agreement with experiment than the result of three dimensional CFD data done by Wang and Widhopf. This result means that the present method can numerically simulate the motion of supersonic jet flow at the initial stage.

Another condition of supersonic het flow is numerically simulated. The Mach number of jet flow is 2.1 and it is fully expanded condition. So there is no pressure difference between jet flow and ambient and no shock cell structures are exist. Fig. 3 shows a two dimensional density contour and no clear shock cell is observed. The supersonic Mach waves which propagate downstream are also observed as shown in Fig. 4.

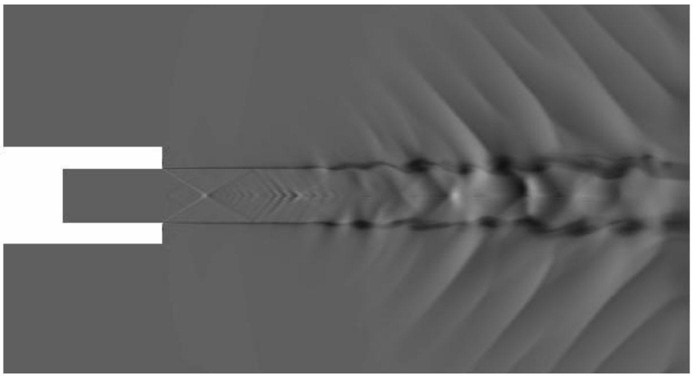

Fig. 3 Density contour of fully expanded supersonic jet (jet Mach number = 2.1)

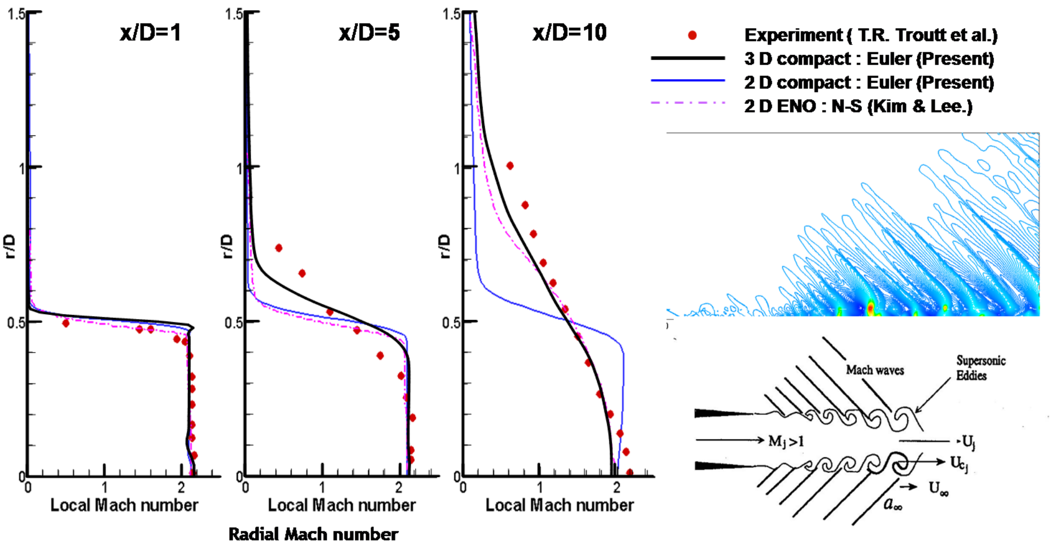


Fig. 4 Averaged Mach number distribution in radial direction at various locations

For more quantitative validation, averaged Mach number distribution in radial direction is calculated at three locations and compared with other results in Fig. 4. Experiments (circular symbol) were performed by T. R. Troutt et al.[12] and two dimensional ENO data (dashed dot line) are the results of N-S simulation and were performed by Kim and Lee[13]. The results of two dimensional Euler simulation (thin line) are also compared. Just at the nozzle exit (x/D=1), all distributions looks similar since the jet flow is so strong and the initial velocity profile is maintained. As the flow goes down stream, the experimental results show the three dimensional diffusion effect and the jet flow spreads in radial direction since supersonic eddies or vortices are generated and the initial velocity profile is not maintained at downstream. Present three dimensional results and two dimensional results also show similar trend however the results of two dimensional do not change a lot with respect to location. The initial velocity profile is almost maintained at x/D=10 even though supersonic eddies or vortices are generated at downstream in two dimensional Euler simulation. It can be concluded that the effect of three dimensional diffusion is as much important as the effect of viscous term in N-S equation.

Through two flow conditions which has the three dimensional effect, the present numerical method is validated. The present method provides good results for initial motion of jet flow from the beginning and for the averaged properties of jet flow at various locations. So it is concluded that the present method can simulate various modes of screech tone which are generated from supersonic jet around the nozzle exit.

## 3.2 Transient behavior of screech tones at low jet Mach numbers

It is known that there are various screech modes with respect to jet Mach numbers. At low jet Mach numbers which is less than 1.20, two axisymmetric modes, A1 and A2 modes, are observed. As the jet Mach number increases, three dimensional modes, B and C modes, are observed. The frequencies of modes vary and are suddenly shifted from one mode to another mode with an increase of the jet Mach number.

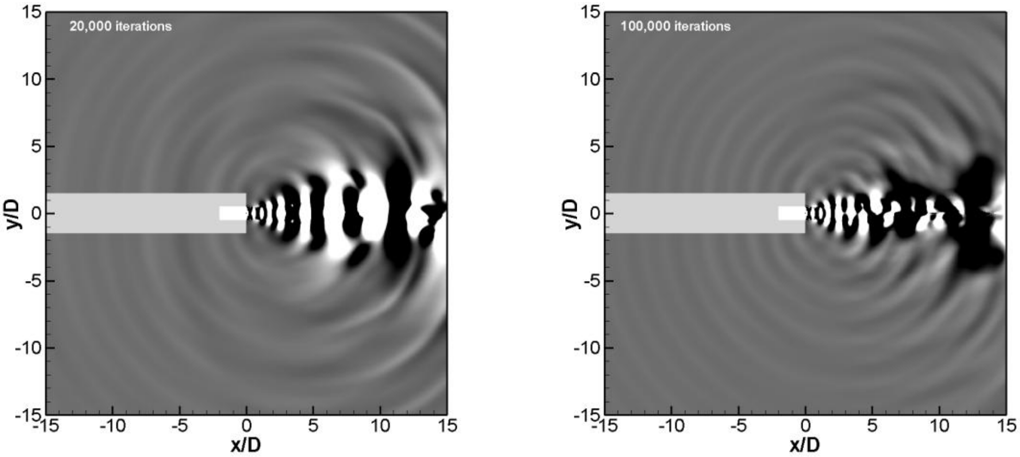


(a) jet Mach number = 1.10

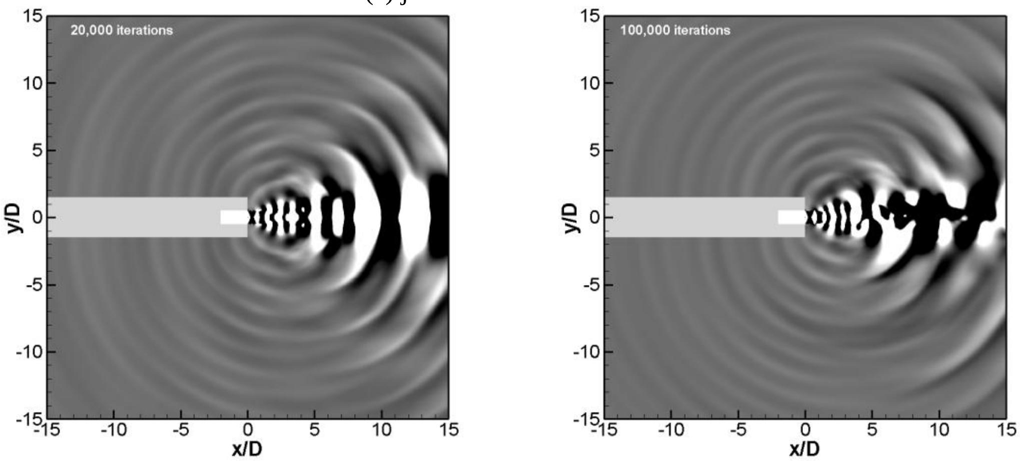


(b) jet Mach number = 1.15

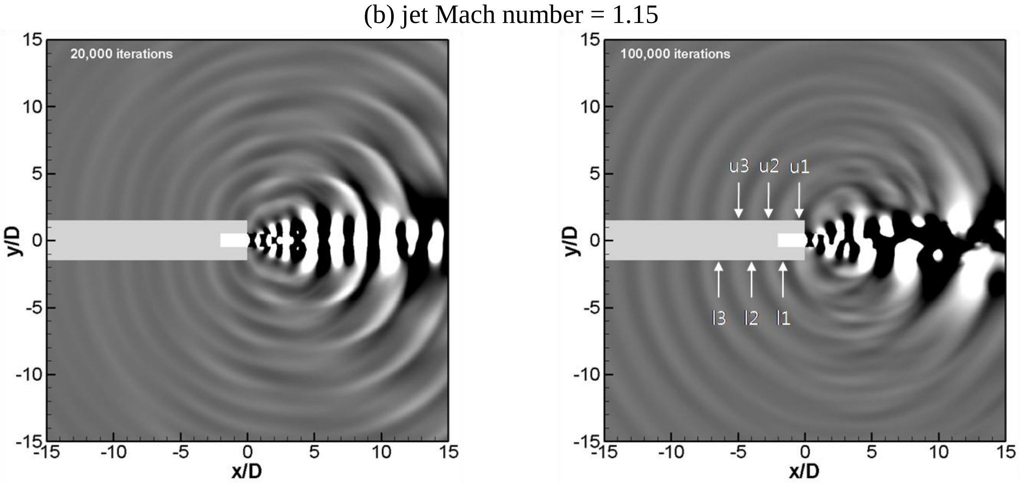


(c) jet Mach number = 1.18

Fig. 5 Comparison of pressure contours for two iteration times in case of three jet Mach numbers ($0.99<p/p_a<1.01$)

Fig. 5 shows the comparison of pressure contours for two iteration times (20,000 iterations and 100,000 iterations) in case of three jet Mach numbers: 1.10, 1.15 and 1.18. At early iterations, every pressure contour shows the axisymmetry along the y/D=0 axis with regardless of jet Mach numbers. However at later iterations, different characteristics are observed with respect to jet Mach numbers. When jet Mach number is 1.10 or 1.15, the screech tones which propagates upstream has the axisymmetric characteristic along the y/D=0 axis even though the jet flow does not show the axisymmetry as shown in right hand side of Fig. 5 (a) and (b). When jet Mach number is 1.18, the screech tones of upper side and lower side clearly show the phase difference. If the first three screech tone waves at upper side are defined as 'u1', 'u2' and 'u3', and at lower side as 'l1', 'l2' and 'l3' as shown in right hand side of Fig. 5 (c), then it is clearly observed that the phase difference between upper waves and lower waves is about 180 degrees or half period. It is also observed that the wavelength of 100,000 iterations is much bigger than that of 20,000 iterations. It can be know that the screech tone is axisymmetric even though the jet flow is not axisymmetric when jet Mach number is less than 1.18 and the screech tone becomes asymmetry as computational time increases when jet Mach number is 1.18.

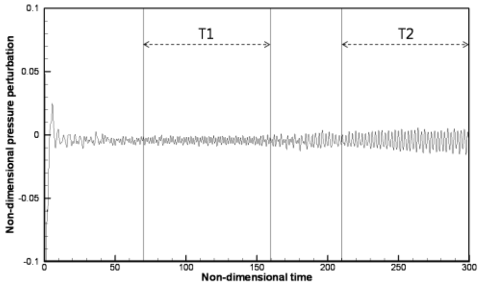


Fig. 6 History of non-dimensionalized pressure signal at the nozzle exit plane

To investigate the generation and the transient behavior of the screech tones when jet Mach number is 1.18, a pressure signal is measures at one position of nozzle exit plane and two non-dimensional time periods T1 and T2 are chosen as shown in Fig. 6. T1 is a period of axisymmetric screech tones and T2 is a period of non-axisymmetric screech tones. Fig. 7 shows the results of Fast Fourier Transform (FFT) for two non-dimensional time periods. At each period, 1024 data are used for FFT. The sampling ratio is 0.075 non-dimensional time so the non-dimensional sampling frequency is about 13.3. The non-dimensional Nyquist frequency is about 6.67 and the non-dimensional frequency resolution is about 0.013.

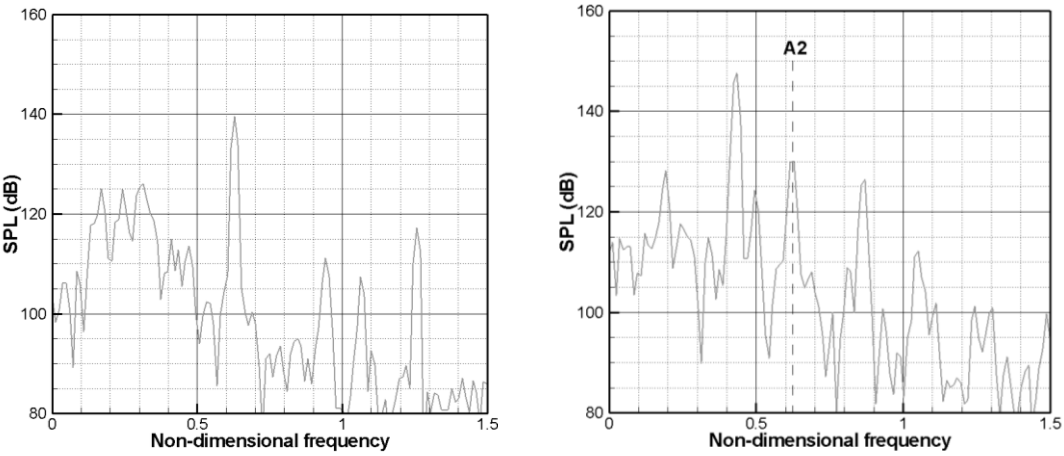


(a) Result of T1 (b) Result of T2

Fig. 7 FFT results of two period T1 and T2

Fig. 7 (a) shows the FFT result of non-dimensional time period T1. The component of non-dimensional frequency equal to 0.625 is dominant, which is axisymmetric and is known as A2 mode. Fig. 7 (b) shows the FFT results of non-dimensional time period T2. The A2 component which is dominant at T1 is shown as dashed line for reference. It is observed that the A2 mode becomes less dominant and another component of lower non-dimensional frequency becomes dominant at T2. This means that the wavelength of dominant component at T2 is bigger than that of dominant component at T1 or A2 mode, which corresponds with the observation in Fig. 5 (c). It can be concluded that the screech tone of three dimensional mode has lower frequency than axisymmetric mode.

### 3.3 Investigation of three dimensional mode of screech tone (B and C mode)

As shown in previous results, screech tones of higher mode are generated when jet Mach number is 1.18. To investigate the characteristics of higher modes, a supersonic jet flow of Mach number equal to 1.43 is numerically simulated. Fig. 8 shows the comparison of density contours at two different iteration times. Like the results of lower jet Mach numbers, the axisymmetric characteristic is observed after 20,000 iterations. And this axisymmetric characteristic disappears and three dimensional effect appears as the computational time increases as shown in Fig. 8 (b). Not only vortices but also shock cell structures inside jet flow show asymmetric characteristics as flow goes downstream.

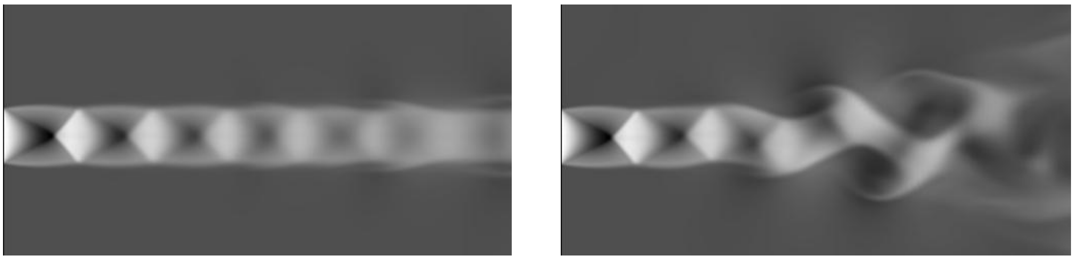

(a) 20,000 iterations (b) 100,000 iterations

Fig. 8 Comparison of density contours for two iteration times when jet Mach number is 1.43

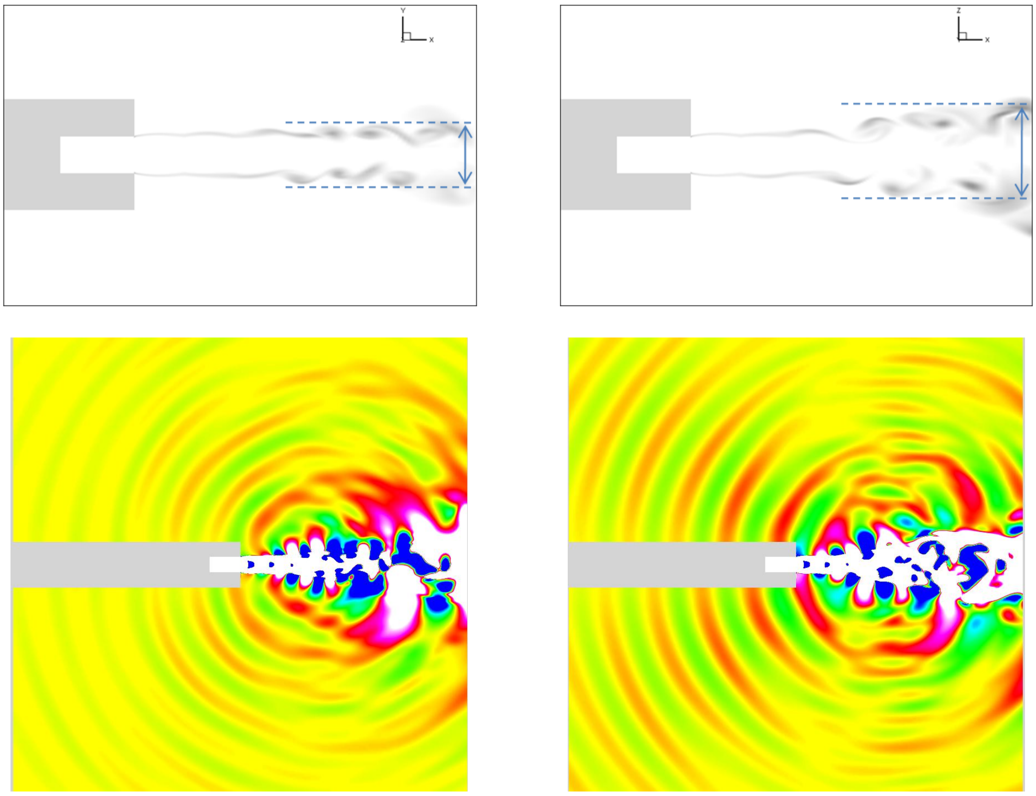

(a) xy plane (b) xz plane

Fig. 9 Vorticity contour (upper figure) and contour of acoustic propagation (lower figure) at two different planes

It is interesting that the asymmetric characteristic shown in Fig 9 (b) is different for different plane. Fig. 9 shows the vorticity contours and contours of acoustic propagation at xy plane and xz plane. The direction of x axis is same as the direction of flow direction and xy plane and xz plane are perpendicular each other.  The size of vortices on xz plane is larger than that on xy plane and the vortices on xz plane spread out more widely than on xy plane. Acoustic waves which propagate upstream, or screech tones, are generated on both planes. However, it is observed that the screech tone on xz plane is much clearer and its wavelength is much bigger.

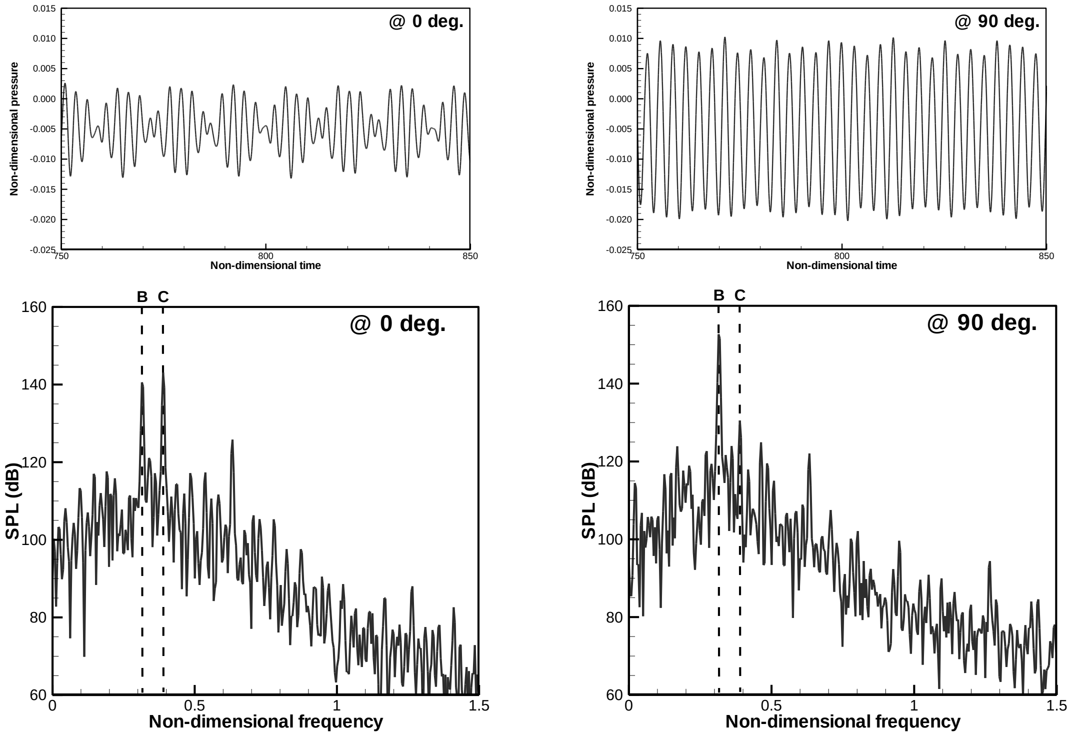


(a) xy plane (b) xz plane

Fig. 10 Non-dimensionalized time history signal and its spectral analysis at two different planes

To investigate the characteristics of screech tones at two planes, non-dimensional time signal was measured at nozzle exit plane and the FFT process was performed with the signal at each plane as shown in Fig. 10. The FFT results in Fig. 10 show that the screech tone at xy plane consists of two components. The component of lower frequency is known as B mode and the component of higher component is known as C mode. And only B mode is dominant at xz plane and the amplitude difference between B mode and C mode is about 20 dB.

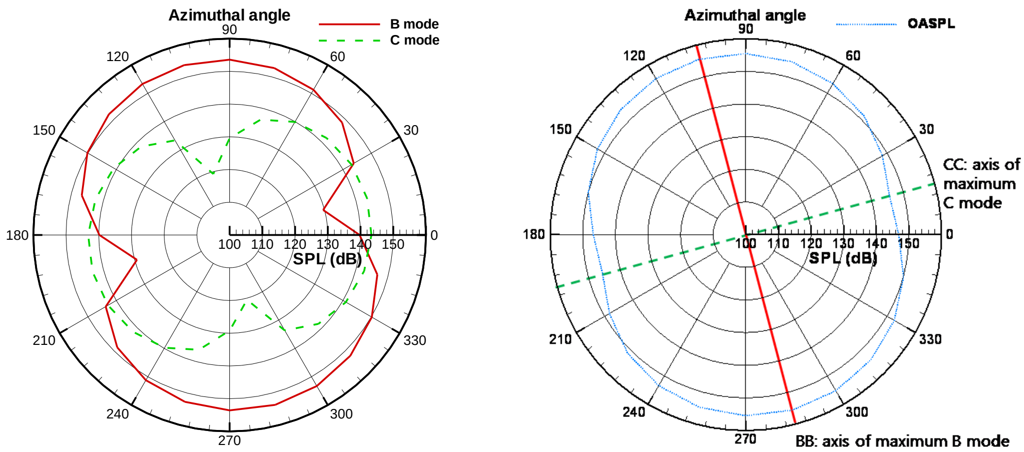


Fig. 11 Directivity of two modes (B and C) and the definition of two planes (BB and CC)

It is clear that different plane has different components of screech tone. This means that the screech tone has directivity and it is shown in Fig. 11. The straight line is the directivity of B mode and the dashed line is the directivity of C mode in the left side figure of Fig. 11. It is observed that the directivities of B mode and C mode are very similar with the directivity of dipole sources and their directivities are perpendicular to each other. To observe the flow behavior which generates B mode and C mode, two planes are defined as shown in the right side figure of Fig. 11. BB plane is a plane at which the amplitude of B mode has maximum value whereas the amplitude of C mode has minimum value. CC plane is a plane at which the amplitude of C mode has maximum value and the amplitude of B mode has minimum value. The maximum amplitude of B mode is about 153 dB at BB plane and the maximum amplitude of C mode is about 143 dB at C plane. So the difference between maximum B mode and maximum C mode is about 10 dB. And BB plane and CC plane are perpendicular each other as shown in Fig. 11.

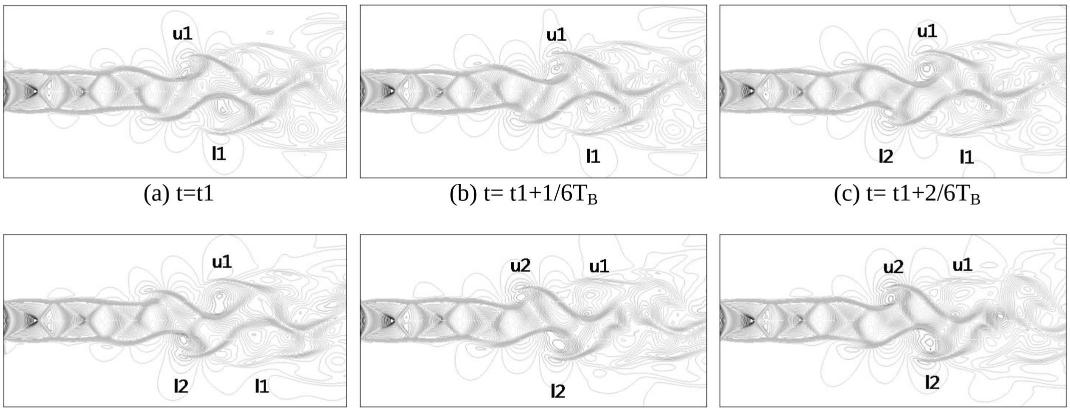


(a) t=t1 (b) t= t1+1/6$T_B$ (c) t= t1+2/6$T_B$

(d) t=t1+3/6$T_B$ (e) t=t1+3/6$T_B$ (f) t=t1+5/6$T_B$

Fig. 12 Variation of density contours during one period of B mode at BB plane

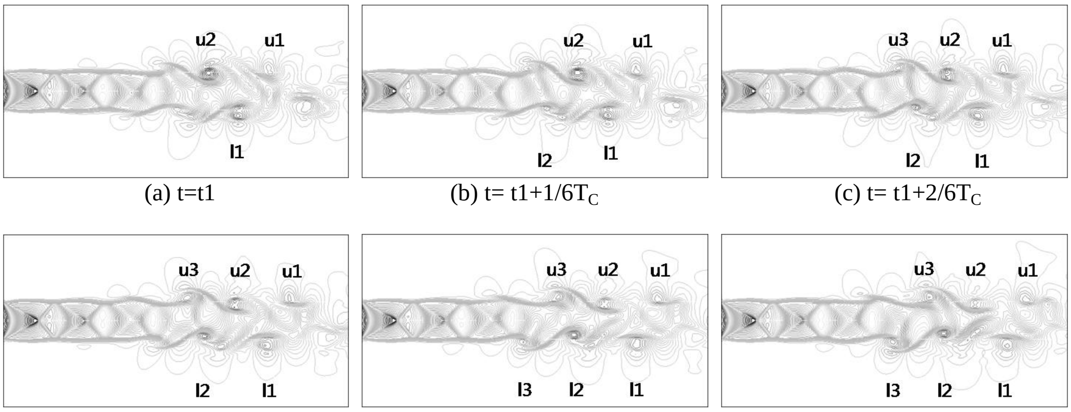


(a) t=t1 (b) t= t1+1/6$T_C$ (c) t= t1+2/6$T_C$

(d) t=t1+3/6$T_C$ (e) t=t1+3/6$T_C$ (f) t=t1+5/6$T_C$

Fig. 13 Variation of density contours during one period of C mode at CC plane

Fig. 12 and 13 show the variations of density contours during one period of B mode and C mode at each plane. The vortices which are generated from upper side are named as ‘u1’ and ‘u2’ and so on. The vortices which are generated from lower side are named as ‘l1’ and ‘l2’ and so on. The upper vortices and the lower vortices are generated by turns at both BB and CC plane. The upper vortex ‘u2’ in Fig. 12 (f) corresponds to the upper vortex ‘u1’ in Fig. 12 (a) and the upper vortex ‘u3’ in Fig. 13 (f) corresponds to the upper vortex ‘u2’ in Fig. 12 (a). It is observed that the size of vortices at BB plane is larger than the size of vortices at CC plane and the length between vortices at BB plane is also larger than the width between vortices at CC plane. This means that the characteristic length of BB mode is longer than that of CC mode and this observation explains why the non-dimensional frequency of B mode is lower than that of C mode since the frequency is in inverse proportion to wavelength. Also the supersonic vortices and shock cell structures shows the flapping motion at both BB and CC plane. The large flapping motion begins from 4th shock cell structures and the width of flapping motion at BB plane is wider than the width of flapping motion at CC plane. This may explain why the maximum B mode is larger than the maximum C mode by 10 dB.

It can be concluded that the B mode is generated by the flapping motion of flow. And the location of maximum perturbation is beyond the 4th shock cell, since the whole shock cell shows strong flapping motion. And the amplitude of C mode is smaller than that of B mode because the flapping motion of C mode is not as strong as that of B mode in this work.

## 3. Conclusions

When the jet Mach number is relatively law, the supersonic jet flow generated screech tone of axisymmetric mode after transient behavior. As the jet Mach number increases, the supersonic jet flow starts to generate the screech tone of three dimensional mode. However, at the initial stage, both the jet flow and the screech tone show axisymmetry even for higher jet Mach number. And the characteristics of asymmetry and three dimensional screech tone are shown as computational time increases. The interaction between vortices and shock cells at the initial stage and the interaction between vortices and shock cells at the later time which shows three dimensional effect are compared each other. The azimuthal variation of three dimensional screech tone is investigated. Two modes can be observed in three dimensional analysis. One is known as B mode, the other is known as C mode. Both B mode and C mode are observed at jet Mach number 1.43 and their azimuthal directivity is also observed. It is observed that the directivities of both B mode and C mode is similar with the directivity of dipole source, however their main directivities or maximum flapping planes are perpendicular to each other.

**ACKNOWLEDGMENTS**

This work was supported by the Space Technology Program of KISTEP (Korea Institute of Science and Technology Evaluation and Planning).

**REFERENCES**

[1] Tam, C. K. W., “Supersonic jet noise,” *Annual Review of Fluid Mechanics*, 1995, 27, 17-43.
[2] Shen, H. and Tam, C. K. W., “Numerical simulation of the generation of axisymmetric mode jet screech tones,” *AIAA Journal*, 1998, 36 (10), 1801-1807.
[3] Kim, Y. S. and Lee, D. J., “Acoustic Properties Associated with Nozzle Lip Thickness in Screeching Jets,” *Journal of Mechanical Science and Technology*, 2007, 21 (5) 764-771.
[4] Freund, J.B., “Acoustic sources in a turbulent jet: a direct numerical simulation study,” AIAA/CEAS Aeroacoustics Conference and Exhibit, Bellevue, WA, 1999, 1-13.
[5] Bogey, C., Bailly, C. and Juve, D., “Computation of the sound radiated by a 3-D jet using large eddy simulation,” AIAA/CEAS, Aeroacoustics Conference and Exhibit, Lahaina, HI, 2000, 2000-2009.
[6] Kim, J. W. and Lee, D. J., “Optimized compact finite difference schemes with maximum resolution,” *AIAA Journal*, 1995, 23 (5), 887-893.
[7] Kim, J. W. and Lee, D. J., “Implementation of boundary conditions for optimized high-order compact scheme,” *Journal of Computational Acoustics*, 1997, 5 (2), 177-191.
[8] Kim, J. W. and Lee, D. J., “Adaptive nonlinear artificial dissipation model for computational Aeroacoustics,” *AIAA Journal*, 2001, 39 (5), 810-818.
[9] Kim, J. W. and Lee, D. J., “Generalized characteristic boundary conditions for computational Aeroacoustics,” *AIAA Journal*, 2000, 38 (11), 2040-2049.
[10] Jorgenson, P. and Loh, C., “Computing axisymmetric jet screech tones using unstructured grids,” 38th AIAA/ASME/SAE/ASEE Joint Propulsion Conference and Exhibit, Indianapolis, Indiana, 2002, AIAA-2002-3889.
[11] Wang, J. C. T., and Widhopf, G. F., "Numerical simulation of blast flow fields using a high Resolution TVD finite volume scheme", *Computers & Fluids*, 1990, 18 (1), 103-137.
[12] Troutt, T. R., and Mclaughlin, D. K., "Experiments on the flow and acoustic propertied of a moderate-Reynolds-number supersonic jet", *Journal of Fluid Mechanics*, 1982, 116, 123-156.
[13] Kim, Y. S., “Analysis of radiated noise from internal duct flow and external jet using high-resolution schemes,” Ph.D. thesis, KAIST, 2001.